THE JOURNAL OF PHYSICAL CHEMISTRY C LETTERS

2008, *112,* 4029−4032
Published on Web 03/06/2008

Photocatalytic Induction of Nanobubbles on TiO_2 Surfaces

Guangxia Shen,[†] Xue Hua Zhang,[‡] Ye Ming,[†] Lijuan Zhang,[†] Yi Zhang,[†] and Jun Hu*[,†,§]

Shanghai Institute of Applied Physics, Chinese Academy of Sciences, Shanghai 201800, Department of Chemical and Biomolecular Engineering and Particulate Fluid Processing Center, University of Melbourne, Melbourne 3010, Australia, and Bio-X Life Science Research Center, College of Life Science and Biotechnology, Shanghai Jiao Tong University, Shanghai 200030 China

Received: December 18, 2007; In Final Form: February 20, 2008

In this work, we investigate the formation of nanobubbles on a surface coated with TiO_2 in an aqueous solution by in situ tapping-mode atomic force microscopy (TMAFM). The TiO_2-coated surface can generate hydrogen through photocatalytic reaction in methanol/water solution when ultraviolet (UV) light (wavelength $\lambda < 400$ nm) is illuminated on the surface. We found that nanobubbles could be produced and existed at the TiO_2/water interface during the TiO_2 photocatalytic process. By employing a combination of techniques, including phase imaging and contact-mode imaging, we could confirm the gas origin of such observed nanobubbles. In addition, the evolution process of nanobubbles at the TiO_2/water interface has also been monitored with time of the photocatalytic reaction.

Introduction

The ubiquitous presence of nanobubbles at hydrophobic surfaces in water has been a controversial topic in surface science. If present, nanobubbles may have significant implications in many important phenomena, such as hydrodynamic forces,[1−4] adsorption of biomolecules at surfaces,[5] formation of complicated crystal nanostructures,[6] microboiling,[7] and design of microdevices.[8] But many reports about the presence of nanobubbles lack reproducibility, thus casting doubt on the claim as to the ubiquitous presence of nanobubbles. In contrast, we established a different approach, deliberately inducing nanobubbles on a surface by the so-called "solvent exchange" method.[9] This new approach enabled us to induce nanobubbles in a highly reproducible manner. The possible mechanism underlying this protocol is that gas supersaturation can be induced during the exchange of the solvents that have different solubilities of gases.[10] Recently, the study from attenuated total reflectance infrared spectroscopy (ATR-FTIR) and surface plasmon resonance (SPR) have provided direct evidence for the gaseous state of the bubbles created by this method.[11] Nanobubbles can also be induced reproducibly by electrochemical reaction[12] or inducing appropriate temperature gradients.[13]

In the current report, we study the formation of nanobubbles via yet another important process: photocatalytic reaction on a TiO_2 surface. Gases, such as H_2, O_2, and CO_2,[14] are often produced in the photocatalytic reaction. It is possible that nanobubbles of these gases can be formed during the reaction process. To the best of our knowledge, the possible effect of nanobubbles on the photocatalytic reaction has not been considered. These nanobubbles may prevent or slow down further photocatalytic reaction because they may physically block the contact between reactants and the catalyst. In this work, we study whether nanobubbles can be formed at the TiO_2 coating interface in aqueous methanol solution by using in situ tapping-model atomic force microscopy (TMAFM). We found that nanobubbles did form during the photocatalytic reactions. We also recorded the increase of nanobubbles at the TiO_2/solution interface with the time of photocatalytic reaction.

Experimental Section

Materials. In our experiments, water was purified with a milli-Q system (Millipore Corp., Boston, MA). Tetraisopropyl orthotitanate (TIPT; $Ti(C_3H_7O)_4$, Fluka) was used as received, and TiO_2 and other chemical regents were obtained from Chinese Chemical Reagent Co. Mica was from S&J Trading Co., New York.

Preparation of TiO_2 Coating. The procedure to coat TiO_2 on the substrate has been reported in our previous work.[15] Here mica was used as the substrate, which is very smooth and suitable for AFM imaging. To make the coating, we prepare a polymeric sol first as below: TIPT and ethyl acetoacetic (EAcAc) were mixed in absolute ethanol, and then water was dropped into the mix solution. Here, the ethanol was solvent and EAcAc was a catalyst and chelating agent. The volume ratio of TIPT/EAcAc/water/ethanol was 1:0.2:1:20. Then the sol was aged at room temperature for 2 days.

The polymeric sol was coated onto a round freshly cleaved mica (diameter 10 mm) by spin coating using a spinning microtechnology apparatus. Twenty microliters of sol was spread on mica at 5000 rpm for 20 s. After the deposition of liquid film, the solvent evaporated rapidly and a solid film formed at ambient conditions through the well-known sol−gel polymerization route. Then the samples were dried in an oven at 150 °C for 30 min. The films were subsequently calcined at a rate

* Corresponding author. E-mail: jhu@sjtu.edu.cn.
[†] Chinese Academy of Sciences.
[‡] University of Melbourne.
[§] Shanghai Jiao Tong University.

10.1021/jp711850d CCC: $40.75

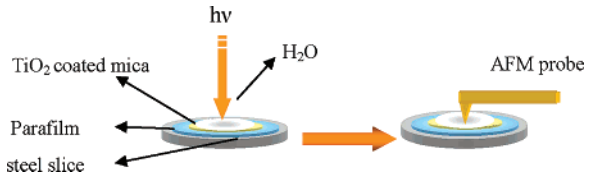

Figure 1. Schematic diagram of photocatalytic setup and AFM image system.

of 100 °C/h to 450 °C and kept at 450 °C for 1 h, and finally the coatings were furnace-cooled. The film thickness measured from the section of SEM image was 89 ± 1 nm.[16]

Observation of Nanobubbles on TiO_2-Coated Surface in Water. The TiO_2-coated mica surface was imaged in water by tapping-mode atomic force microscopy (TMAFM, MultiMode Nanoscope IIIa, Veeco). A closed fluid cell with an O-ring was used. A triangle cantilever (NP-S, Digital Instruments Veeco Metrology Group) with a normal spring constant of 0.58 N/m was used for the tapping-mode imaging in liquid. Before use, the cantilever and fluid cell were cleaned carefully with ethanol and water in sequence and then were dried with nitrogen gas. We followed Zhang's procedure to image bubbles by tapping-mode AFM image in liquid.[17,18] The drive frequency for the cantilever in water was set at 6.0−9.5 kHz. At least five different areas on the surface were imaged. The height and phase images were captured simultaneously during AFM imaging. The ambient temperature for all experiments was 25 ± 2 °C.

Photocatalytic Experiments. Photocatalytic experiments were carried out on a clean bench that was equipped with a UV lamp of 25 W. Figure 1 shows the schematic diagram of the photocatalytic setup and AFM image system. It was well known that the TiO_2 coatings would get superhydrophilic after UV illumination.[19] To prevent the spill onto the AFM scanner under the substrate, we inserted a hydrophobic Parafilm between the steel slice stabilized on the piezo by a magnet and the TiO_2-coated mica. The diameters of three round plates are steel slice > Parafilm > TiO_2-coated mica > O-ring. About 120 μL of l vol % methanol in water solution was pre-degassed at 0.1 atm for 2 h and then was promptly injected into the AFM liquid cell. (The reaction rate of 1 vol % methanol solution is suitable for detecting the evolution process of the nanobubbbles by in situ AFM.) Before the photocatalytic reaction, the TiO_2-coated surface was imaged by TMAFM. Then the coatings were moved from AFM head to the clean bench and the UV light was vertically mounted about 3−5 cm far from the top of liquid drop. TMAFM recorded the features on the surface after UV irradiating every 10 min. The evolution of the nanobubbles at the coating interface was investigated systematically with photocatalytic water-splitting time. Control experiments, using a hydro-philic mica film, were carried out the photocatalytic experiments at the same conditions (see Supporting Information).

Results and Discussion

Characterization of TiO_2 Coatings in Air. The freshly cleaved mica surface is very small. After the TiO_2 film is coated, the representative AFM images in air (Figure 2a and b) show that the surface was coated with the TiO_2 uniformly and densely. The TiO_2 film was very flat with a root-mean-square (rms) roughness of ±1 nm. Figure 2c and the marked region in Figure 2a show that the coatings were made up of spherical nanoparticles with diameters of 5 to 15 nm. Our previous work has confirmed that the crystallinity of titanium oxide prepared by this method was anatase phase by X-ray diffraction,[16] which has a high photocatalytic activity.

TiO_2-Coated Surface in Aqueous Solution With and Without the UV Illumination. Before UV illumination, the TiO_2-coated surface was imaged in 1 vol % methanol solution by tapping-mode AFM. The representative TMAFM images obtained at 25 ± 2 °C are shown in Figure 3a and b. Similar to what we observed in air, the surface is very smooth with an rms of ±1 nm. Meanwhile, there is no contrast in the phase image (Figure 3b), which means that the surface is homogeneous. The surface is very stable in the solution and can remain unchanged for at least a few hours.

However, after the UV light was irradiated to the TiO_2 coatings in 1 vol % methanol aqueous solution for 1/2 h, many nanoscale features could be observed at the interface between TiO_2-coated mica and the aqueous solution, as shown in Figure 3c. The phase image of the same area shows the distinctive contrast between these nanoscale features and the substrate (Figure 3d). Because the phase image is very sensitive to variations of material properties such as elasticity, adhesion, and viscoelasticity, the contrast in Figure 3d indicates that those features are different in nature from the hard particles of TiO_2 shown in Figure 2. So these features are newly formed in the photocatalytic reaction. Given the large amount of gases created in the reaction, we believe that those nanoscale entities are actually nanobubbles that are formed from the supersaturation of the gases. It has been reported that nanobubbles at solid/water interfaces reproducibly form when the supersaturation of gases is created, such as by solvent exchange, electrochemical reaction, or temperature gradient. So it is not surprising that the bubbles can be formed during the photocatalytic reaction.

To further confirm the features are nanobubbles, we image the surface of TiO_2 coating after UV illumination in contact mode. Figure 3e and f show that there is no contrast in either the height or lateral force images. This is consistent with a previous report that nanobubbles are difficult to observe in contact mode.[20]

Morphology of the Nanobubbles. The height of the nanobubbles ranged from a few nanometers to 80 nm, and the lateral dimension varied from several hundred nanometers to a few hundred micrometers. So, they are very flat. From the TMAFM image of the nanobubbles, we estimated the contact angle of the nanobubbles by the procedure in earlier works.[19] The value of the contact angles was about 120°, which is very different from the macroscopic contact angle of 1 vol % methanol aqueous solution on the TiO_2 surface. This is consistent with a previous report about the distinctive difference between the contact angle of nanobubbles and the macroscopic counterpart.

Evolution of Nanobubbles on the TiO_2 Surface. Figure 4 a−d is the series of the height images of surfaces during the TiO_2 photocatalyic process. As described above, no nanobubbles were observed on the TiO_2-coated surface in 1 vol % methanol solution before UV illumination (Figure 4a and b). Nanobubbles began to form after applying UV light for about 10 min (Figure 4c), and both the numbers and the apparent volume of the nanobubbles increased with time of the UV illumination (Figure 4d). When the photocatalytic reaction persisted for 30 min (from Figure 3c and d), the monitoring of nanobubbles by the TMAFM was getting more and more difficult. Many nanobubbles accumulated rapidly at the TiO_2 coating, in the solution, and near or on the probe and formed big bubbles that interfered with the laser beam and resulted in large instability during TMAFM imaging. Figure 3c shows that more nanobubbles are formed after longer radiation times.

We stopped the photocatalytic reaction after 20 min and found that the nanobubbles have a lifetime of about several hours. It

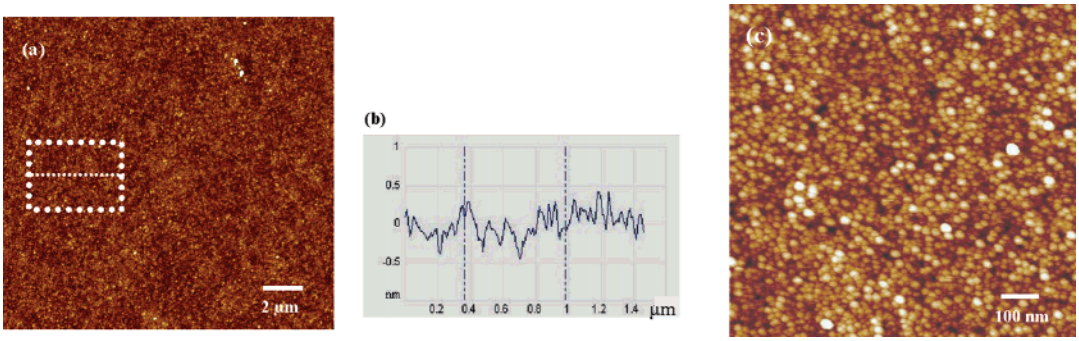

Figure 2. Representative TMAFM image and section analysis of the TiO_2-coated surface in air: Vertical size: 10 nm. (a) Height image; (b) section analysis of the marked region in Figure 2a; (c) the zoom of the Figure 2a.

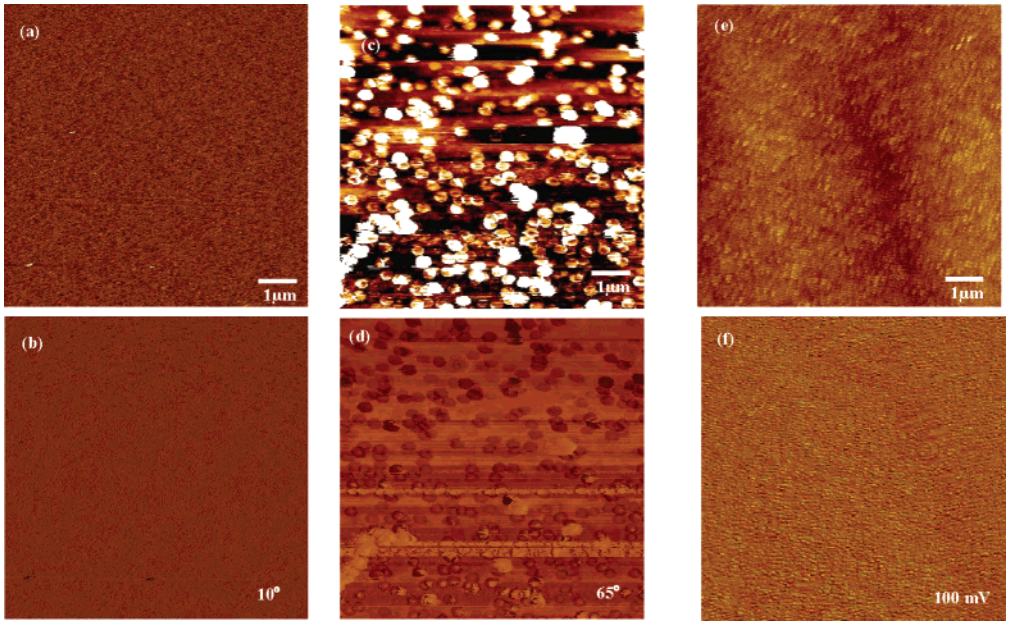

Figure 3. (a−d) TM-AFM height and phase images of TiO_2 coatings in the 1 vol % methanol solution. (a) Height image and (b) phase image before UV light; (c) height image and (d) phase image under UV light after 30 min. (e and f) AFM image of the same sample by contact mode in the 1 vol % methanol solution.

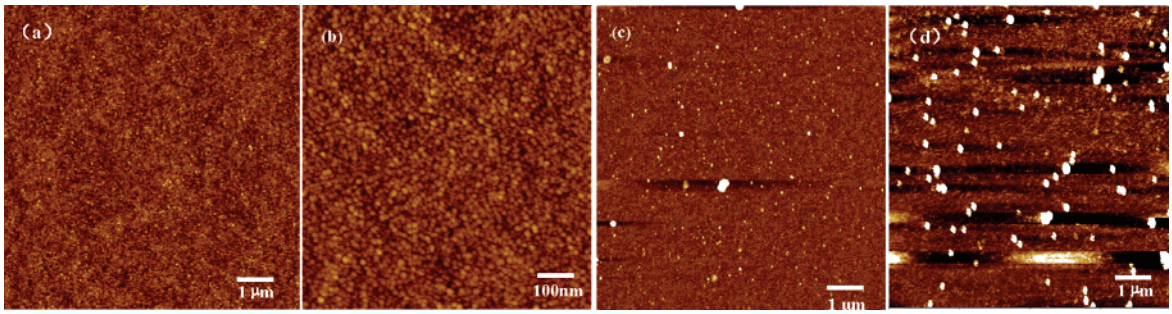

Figure 4. TM-AFM height images showing the evolution process of nanobubbles at the TiO_2 coating interface with time of photocatalysis. (a and b) 0 min; (c) 20 min; (d) 30 min. Z range: (a and b): 10 nm; (c and d): 20 nm.

is surprising that those bubbles can stay so long, although there is always the remaining puzzle about the long lifetime of nanobubbles, even for air nanobubbles. If our nanobubbles are only formed by the gases (hydrogen or carbon dioxide) produced in the photocatalytic reaction, then they should disappear in even short time because the partial pressure of these gases in atmosphere is quite low and the gases can diffuse away from bubbles very soon. We suspect that the temperature fluctuation during the photocatalytic reaction may also facilitate the supersaturation of dissolved air and form some air bubbles (see Supporting Information).

Implication of Nanobubbles on the Photocatalytic Reaction. The fact that the dense nanobubbles in the AFM images covering the TiO_2-coated surface and the bubbles have quite long lifetimes suggests that the nanobubbles may contribute to the inhibition of the further photocatalytic reaction. Because the most important factor for the chemical activity of a catalyst is the number of active sites, the existence of nanobubbles must have decreased the total available surface area of the TiO_2 coatings and may hinder the photogenerated electrons or holes to induce the reaction.[21] Many researchers have historically realized that it is a main reason for the defects in the

electrodeposited coating that electrogenerated gas, in the form of bubbles and sticking to the interface of electrodes, covered the corresponding surface of the electrodes and hindered the shift freely of charge at the interface. For example, Tsai et al. elegantly demonstrated that adsorbed hydrogen bubbles were responsible for bubble-shaped microscale defects.[22] Wang and co-workers observed that water-electrolysis-induced mineralization led to the formation of submicrometer vaterite tubes at the cathode surface, and they explained that the formation of nanocrystalline vaterite cylinders may be a combined effect of hydrogen bubbles as the template and the continuous movement of the bubble front.[23] But the photocatalytic process was very different from the electrochemical process. In the photocatalytic process the electric field did not exist, so photogenerated electron and hole cannot shift at the surface of bubbles. Thus, nanobubbles absorbed at the photocatalyst surface can cause the partial deactivation not only by reducing the area of the photocatalyst but also by hindering electron or holes shifting at the interface of the TiO_2 photocatalyst. These may be important factors of the lower efficiency of the TiO_2 photocatalyst. Unfortunately, by being degassed or ultrasonically cleaned, the bubbles cannot be removed from the interface of the TiO_2 photocatalyst. The effects of nanobubbles on TiO_2 photocatalysis will be studied systematically in our next work.

Conclusions

We have revealed that nanobubbles could be produced and existed at the TiO_2/water interface during the photocatalytic process by using TMAFM. The number and volume of nanobubbles increased with time during the photocatalytic reaction. These nanobubbles can remain at the interface for at least a few hours after the reaction. This finding may have significant implication on the photocatalytic reaction of TiO_2 because the existence of those nanobubbles may inhibit the reaction induced by the photogenerated electron or hole and lead to the low efficiency of TiO_2 photocatalytic reaction, an alternative possibility for the phenomenon of saturation, which has never been considered in this field.

Acknowledgment. We gratefully appreciate financial support from the National Natural Science Foundation of China (10335070, 60537030, 10474109), the Chinese Academy of Sciences, the Shanghai Municipal Commission for Science and Technology Commission (0552 nm033, 03DZ14025), Shanghai Rising-Star Program, the Ministry of Science, Technology of China, and the post-PhD fund of Shanghai and Kuancheng Wang fund of Chinese Academy of Sciences. X.H.Z. acknowledges ARC for the financial support (Australian Postdoctoral Fellowship DP0880152) and the Particulate Fluids Processing Centre (an ARC Special Research Centre) for travel support.

Supporting Information Available: Control experiments showing the effect of a hydrophillic surrounding, temperature gradients, and UV light on the formation of nanobubbles and photocatalytic mechanism of TiO_2 coatings. This material is available free of charge via the Internet at http://pubs.acs.org.

References and Notes

(1) de Gennes, P. G. *Langmuir* **2002**, *18*, 3413−3414.
(2) Dammer, S. M.; Lohse, D. *Phys. Rev. Lett.* **2006**, *96*, 206101.
(3) Tyrrell, J. W. G.; Attard, P. *Langmuir* **2002**, *18*, 160.
(4) Craig, V. S. J.; Ninham, B. W.; Pashley, R. M. *Langmuir* **1999**, *15*, 1562.
(5) Wu, Z. H.; Zhang, X. H.; Zhang, X. D.; Gang, L.; Sun, J. L.; Zhang, Y.; Li, M. Q.; Hu, J. *Surf. Interface Anal.* **2005**, *37*, 797−801.
(6) Tsai, W. L.; Hsu, P. C.; Hwu, Y.; Chen, C. H.; Chang, L. W.; Je, J. H.; Lin, H. M.; Groso, A.; Margaritondo, G. *Nature* **2002**, *417*, 139−139.
(7) Thomas, O. C.; Cavicchi, R. E.; Tarlov, M. J. *Langmuir* **2003**, *19*, 6168−6177.
(8) Paxton, W. F.; Kistler, K. C.; Olmeda, C. C.; Sen, A.; St Angelo, S. K.; Cao, Y. Y.; Mallouk, T. E.; Lammert, P. E.; Crespi, V. H. *J. Am. Chem. Soc.* **2004**, *126*, 13424−13431.
(9) Lou, S. T.; Gao, J. X.; Xiao, X. D.; Li, X. J.; Li, G. L.; Zhang, Y.; Li, M. Q.; Sun, J. L.; Li, X. H.; Hu, J. *Mater. Charact.* **2002**, *48*, 211−214.
(10) Zhang, X. H.; Zhang, X. D.; Shi, T. L.; Zhang, Z. X.; Sun, J. L.; Hu, J. *Langmuir* **2004**, *20*, 3813−3815.
(11) Zhang, X. H.; Khan, A.; Ducker W. A. *Phys. Rev. Lett.* **2007**, *98*, 136101−1∼4.
(12) Zhang, L. J.; Zhang, Y.; Zhang, X. H.; Li, Z. X.; Shen, G. X.; Ye, M.; Fan, C. H.; Fang, H. P.; Hu, J. *Langmuir* **2006**, *22*, 8109−8113.
(13) Zhang, X. H.; Zhang, X. D.; Sun, J. L.; Zhang, Z. X.; Li, G.; Fang, H. P.; Xiao, X. D.; Zeng, X. C.; Hu, J. *Langmuir* **2007**, *23*, 1778−1783.
(14) Ashokkumar, M. *Int. J. Hydrogen Energy* **1998**, *23* (6), 427−438.
(15) Shen, G. X.; Chen, Y. C.; Lin, C. J. *Thin Solid Films* **2005**, *489*, 130−136.
(16) Shen, G. X.; Chen, Y. C.; Lin, C. J. *Corrosion* **2005**, *61*, 943−950.
(17) Zhang, X. H.; Maeda, N.; Craig, V. S. J. *Langmuir* **2006**, *22*, 5025−5035.
(18) Zhang, X. H.; Gang, L.; Maeda, N.; Hu, J. *Langmuir* **2006**, *22*, 9238−9243.
(19) Wang, R.; Hashimoto, K.;Fujishima, A.; Chikuni, M.; Kojima, E.; Kitamura, A.; Shimohigoshi, M.; Watanabe, T. *Nature* **1997**, *388*, 431−435.
(20) Zhang, X. H.; Wu, Z. H.; Zhang, X. D.; Li, G.; Hu, J. *Int. J. Nanosci.* **2005**, 399−407.
(21) Grätzel, M. *Nature* **2001**, *414*, 338−344.
(22) Tsai, W. L.; Hsu, P. C.; Hwu, Y.; Chen, C. H.; Chang, L. W.; Je, J. H.; Lin, H. M.; Groso, A.; Margaritondo, G. *Nature* **2002**, *417*, 139−139.
(23) Fan, Y. W.; Wang, R. Z. *Adv. Mater.* **2005**, *17*, 2384−2388.